Ultrasonic wave propagation through lime mortars: an alternative and non-destructive tool for textural characterization

Anna Arizzi, Javier Martínez-Martínez & Giuseppe Cultrone

Materials and Structures

ISSN 1359-5997
Volume 46
Number 8

Mater Struct (2013) 46:1321-1335
DOI 10.1617/s11527-012-9976-1

Springer

Materials and Structures (2013) 46:1321–1335
DOI 10.1617/s11527-012-9976-1

ORIGINAL ARTICLE

Ultrasonic wave propagation through lime mortars: an alternative and non-destructive tool for textural characterization

Anna Arizzi · Javier Martínez-Martínez · Giuseppe Cultrone

Received: 18 October 2011 / Accepted: 16 November 2012 / Published online: 27 November 2012

Abbreviations

Mortar components, names and proportions

1:2, 1:3, 1:4, 1:6	Binder-to aggregate proportion (by weight) used in mortars
B/A	Binder-to-aggregate ratio
CA	Calcareous aggregate with continuous grading
CC	Mortar with calcitic lime and calcareous aggregate with continuous grading
CD	Mortar with calcitic lime and calcareous aggregate with discontinuous grading
CDA	Calcareous aggregate with discontinuous grading
CL	Calcitic lime
CS	Mortar with calcitic lime and siliceous aggregate with discontinuous grading
SA	Siliceous aggregate with discontinuous grading
w/c	Water-to-cement ratio

Techniques and parameters

A_e	Maximum amplitude emitted by the transmitter sensor
A_{mx}	Maximum amplitude registered by the receptor sensor
α_s	Spatial attenuation of ultrasonic primary wave
C	Ultrasonic wave velocity
E	Young's modulus
FESEM	Field emission scanning electron microscopy
I_{CD}	Carbonation degree index
ITZ	Interfacial transition zone
L	Length of the sample
MIP	Mercury intrusion porosimetry
μ	Poisson's ratio
OM	Polarized optical microscopy
PSD	Pore size distribution
R	Reflection coefficient
RH	Relative humidity
ρ	Density
T	Temperature
v_p	Propagation velocity of ultrasounic primary wave
v_p^a	Propagation velocities within the aggregate

A. Arizzi (✉) · G. Cultrone
Departamento de Mineralogía y Petrología, Universidad de Granada, Campus Fuentenueva s/n, 18002 Granada, Spain
e-mail: arizzina@ugr.es

J. Martínez-Martínez
Laboratorio de Petrología Aplicada, Departamento de Ciencias de la Tierra y del Medio Ambiente, Universidad de Alicante, 03080 Alicante, Spain

v_p^m	Propagation velocities within the matrix
χ^a	Relative volumes of sample aggregate
χ^m	Relative volumes of sample matrix
XRD	X-ray diffraction
Z	Acoustic impedance

1 Introduction

The non-destructive evaluation of mortars is a major issue for estimating the quality, durability and characteristics of pieces in which samples cannot be collected. For example, the study of mortars employed in architectural heritage requires the use of techniques as low invasive as possible. Among all non-destructive testing methods available, the ultrasonic waves is, probably, the most used tool due to the possibility of determining the elastic properties (such as Young Modulus), and also of characterizing micro-structural properties of materials (porosity, grain size or micro-cracks). On the other hand, the correct interpretation of ultrasonic signals is difficult because these micro-structural aspects have different effects on wave propagation, i.e. on velocity and/or attenuation [1]. Consequently, knowing the influence of a specific factor (for example: porosity) on wave velocity or attenuation is very difficult and requires a deep study by means of both empirical and numerical approximations, and only when this influence is completely understood it will be possible to assess mortar characteristics from ultrasonic data with enough exactitude.

The most crucial parameter affecting mortar quality (in terms of its durability) is the water dosage [2], because it is directly related to the pore system characteristics (quantity, size and connectivity of pores), and, as a consequence, it determines the water accessibility as well as the mortar resistance against salt crystallization processes [3]. Several works have been carried out to assess the porosity and the strength of mortars and concretes by means of the use of ultrasounds [4–9]. However, the effects of porosity on ultrasounds are disguised by other wave disruptions caused by aggregates, for example. In fact, the ultrasonic signal obtained after its propagation through the mortar is the result of the initial signal modified by the scattering and the delay caused by pores and aggregate. Moreover, mortars with different aggregate content, mineralogy and grading can be elaborated, and they will have different ultrasonic response.

In the case of mortars and concretes, ultrasonic test may be also useful to study the changes in mechanical properties and microstructure caused by hardening. Generally, carbonation and hydration processes produce an increase in mechanical strength and compactness that determine a proportional increase in the velocity of propagation of longitudinal waves, as well as to a decrease in the anisotropy of the sample [7]. However, the great majority of these studies are focused on cement mortars and concrete, whilst a lack of information exists about the factors that influence the propagation of ultrasonic waves within lime-based mortars. In fact, the latter are characterized by a hardening process (i.e. carbonation) that is much slower in time with respect to the hydration reactions that occur in cement mortars and concrete. Initially, a lime-based mortar is composed of aggregates surrounded by a matrix, in which the main mineralogical phase is portlandite ($Ca(OH)_2$), although small quantities of calcite ($CaCO_3$) can be present as a result of a previous slight carbonation of the lime. The carbonation of a lime-mortar takes place when CO_2 dissolves in the condensed water and reacts with dissolved portlandite. This reaction results in the precipitation of calcium carbonate, due to the rapid supersaturation with respect to $CaCO_3$ in the solution existing in the mortar pores [10–13]. As it has been commented above, the carbonation process is much slower in time than the hydration of cement components, and in fact, portlandite has been detected in Roman mortars after more than 2,000 years after their elaboration. The hardening products (calcite in lime-based mortars, aluminates and silicates hydrated phases in cement and concrete) do not produce the same mineralogical ad microstructural changes in the mortars matrix, with the consequence that the ultrasonic response within lime mortars cannot be correctly interpreted only on the basis of the previous studies on cement mortars and concrete.

The aim of this study is to clarify the influence of mineralogy, grading and dosage of the aggregate on the propagation velocity and the spatial attenuation of P waves within lime-based mortars. To this purpose, four binder-to-aggregate ratios and two aggregates with different composition (siliceous and calcareous) and grading (continuous and discontinuous) were used for the preparation of six types of lime mortars. Differences in mortar microstructure and mineralogy are considered to understand the differences in the

Table 1 Proportions used during the preparation of the six types of mortar

Mortar name	Aggregate	B/A	B	A	W/TOT
CC1:2	CA	1:0.65	60.4	39.6	29.5
CC1:3	CA	1:1	50.4	49.6	31.3
CC1:4	CA	1:1.3	43.3	56.7	24.0
CC1:6	CA	1:2	33.2	66.8	20.0
CD1:3	CDA	1:1	50.4	49.6	27.0
CS1:3	SA	1:1	50.6	49.4	26.5

B/A binder-to-aggregate ratio by volume, *B* proportion of the binder expressed in % by volume; *A* proportion of the aggregate expressed in % by volume, *W/TOT* water amount expressed in % of the total weight

values of propagation velocity and attenuation of P waves. Moreover, the evolution of elastic properties during the carbonation process of lime-based mortars was considered as an important point to study. In order to evaluate this evolution, textural and mineralogical characterization of each mortar type were carried out as well as ultrasonic measurements of every sample, at 7, 10, 15, 60 and 730 days since mortar elaboration.

2 Materials and methods

2.1 Mortars components and preparation

A calcitic dry hydrated lime (CL90S, [14]) was used for the preparation of six types of mortars, with different proportion, as shown in Table 1. Three types of aggregate were used: a calcareous one with both continuous (CA, $0.063 < \phi < 1.5$ mm) and discontinuous (CDA, $0.1 < \phi < 0.8$ mm) grading, and a siliceous one, with a discontinuous grading (SA, $0.1 < \phi < 0.5$ mm). The continuous and discontinuous curves of the aggregates are shown in Fig. 1. CDA presents the same discontinuous curve as SA, although their biggest granulometric fractions differ slightly.

CA was used to prepare mortars with increasing aggregate content, corresponding to the following binder-to-aggregate ratios by weight (B/A): 1:2, 1:3, 1:4 and 1:6 (mortars named CC1:2, CC1:3, CC1:4 and CC1:6 in Table 1). Table 1 also shows the ratios by volume corresponding to each mixture. Mortars with CDA and SA were prepared with a unique B/A ratio, equal to 1:3 by weight (mortars named CD and CS, Table 1). The amount of water (i.e. kneading water)

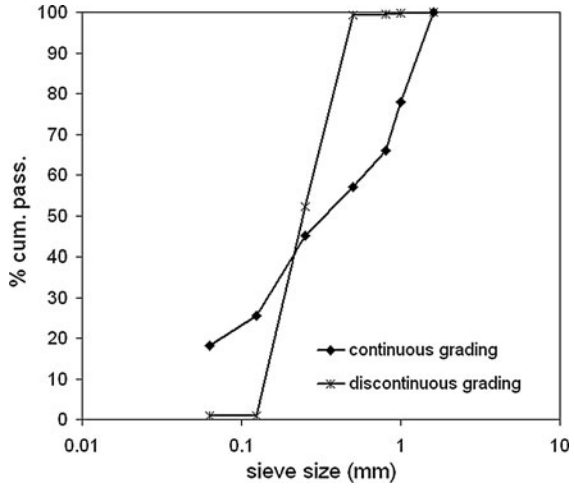

Fig. 1 Grading curves representing the cumulative percentage (% cumul. Pass.) of calcareous and siliceous aggregates grains passing from each sieve size (in log mm)

used in each mortar (Table 1) was established in order to obtain mortars with plastic consistence, which corresponded to a flow comprised between 145 and 150 mm [15].

After mixing, mortars were left during 7 days in normalized steel moulds ($4 \times 4 \times 16$ cm) at RH $= 60 \pm 5$ % and $T = 20 \pm 5$ °C and after demoulding, they were cut in prisms of $4 \times 4 \times 5$ cm. In total, 54 mortar samples were tested in this study (nine of each mortar type) and they were kept at the same temperature and relative humidity during carbonation.

2.2 Textural and mineralogical characterization

2.2.1 Optical and electronic microscopy (OM and FESEM)

The observation of mortars texture and microstructure (morphology, cohesion, porosity) was carried out on thin sections by means of a polarized microscope (OM) (Olympus BX-60) equipped with digital microphotography camera (Olympus DP10). Mortars fragments, previously dried, were carbon-coated and analysed by using a Leo-Gemini 1530 field emission scanning electron microscopy (FESEM).

2.2.2 Mercury intrusion porosimetry (MIP)

Open porosity (P_o, %) and pore size distribution (PSD, in a range of $0.002 < r < 200$ μm) were determined

by means of a Micrometics Autopore III 9410 porosimeter. Three measurements per mortar type were performed on samples with 15, 60 and 730 days (2 years) of carbonation. Mortar fragments of ca. 2 cm^3 were oven-dried for 24 h at 60 °C before the analysis.

2.2.3 X-ray diffraction (XRD)

The identification and quantification of the mineralogical phases of mortars was carried out by means of a Panalytical X'Pert PRO MPD, with automatic loader. Analysis conditions were: radiation CuK_α ($\lambda = 1.5405$ Å), 4–70° 2θ explored area, 45 kV voltage, 40 mA current intensity and goniometer speed using Si-detector X'Celerator of 0.01° 2θ/s. The interpretation and quantification of the mineral phases was performed by using the X-Powder software package [16]. The decrease in portlandite content was taken as reference to estimate the carbonation degree of mortars (I_{CD}, %).

The analysis was performed at different intervals of time: 7, 10, 15 and 60 days and 2 years of carbonation.

2.3 Ultrasound measurements

A Panametrics HV Pulser/Receiver 5058 PR coupled with a Tektronix TDS 3012B oscilloscope was used to perform the ultrasonic tests in transmission-reception mode. A couple of non-polarized piezoelectric transducers was used and a visco-elastic couplant was applied to ensure a good coupling between the transducers and the sample (EKO gel). The frequency of both transducer couples was centred at 1 MHz. This frequency is higher than the 20–150 kHz recommended by the European standard [17] and it was used both to enhance the interaction between the mechanical waves and the textural elements of the material and to increase the resolution. Ultrasonic measurements were carried out on six prisms (40 × 40 × 50 mm) of each mortar samples. This geometry allowed carrying out the test along three directions, one perpendicular and two parallel to the compaction plane. Ultrasonic measurements were performed at the following intervals of time: 8, 10, 15, 60 and 730 (2 years) days of carbonation. From the ultrasonic measurements we obtained propagation velocity (v_p) and spatial attenuation (α_s) values. The former parameter (v_p) was determined as the ratio between the specimen length and the transit time of the pulse. The latter (α_s) quantifies the energy lost during the wave propagation through the material [18]. This quantification was carried out by comparing the amplitude of the signal emitted by the transmitter sensor and the amplitude of the signal received by the receptor. Moreover, spatial attenuation was normalised according to the distance between transmitter and receptor. The α_s value (in dB/cm) was calculated as:

$$\alpha_s = \frac{20 \log\left[\frac{A_e}{A_{mx}}\right]}{L} \quad (1)$$

where A_e is the maximum amplitude emitted by the transmitter sensor, A_{mx} is the maximum amplitude (in absolute values) registered by the receptor sensor, and L is the length of the sample.

3 Results and discussion

3.1 Texture and porosity of the mortars samples

A mortar system is characterized by the presence of aggregate grains surrounded by a matrix in continuous transformation. In fact, since the first hours of curing at standard conditions water evaporation takes place. This first step of mortar life, named drying process, affects importantly the matrix texture, because it produces a high amount of pores in the mortar, as observed in CC1:2, CC1:4 and CC1:6 (Fig. 2) in the form of occasional shrinkage fissures and rounded pores that are more or less big depending on the amount of water [13]. The values of open porosity measured by MIP after 15 days since mortars elaboration are comprised between 30 and 40 % (Table 2) and are lower in mortars with decreasing content of lime. The differences among these values can be linked to the amount of kneading water used in each mix, as also found by Arandigoyen et al. [13] for lime pastes. In fact, CC1:3, which was prepared with the biggest amount of water (Table 1), shows value of open porosity among the highest (Table 2), while CC1:6 mortar presents the lowest porosity (Table 2), because of the least amount of water used for its preparation, followed by CC1:4. When we consider mortars prepared with the same binder-to-aggregate ratio (1:3), CD1:3 shows the lowest porosity, followed by CS1:3 and CC1:3 (Table 2). Notice how in the case of CS mortar there is no relationship between the

amount of water (Table 1) and the porosity, as in CC and CD. The reason of this discrepancy stays in the different morphology of the siliceous aggregate, which is not porous (Fig. 3a) and, consequently, it does not absorb a part of the added water, as it occurs with the calcareous aggregate that presents pores and many fissures (Fig. 3b). After mixing, this water remains free in the CS mortar paste and it is likely to evaporate faster than in the other mortars during drying, thus producing a porosity bigger than the expected (Table 2).

After 2 years of carbonation, the values of porosity (Table 2) decreases in all mortars, by around 2–5 %, whilst it remains almost unvaried in CC1:3 mortar. The porosity decreases due to the growth of new-formed calcite that has a bigger volume than portlandite and fills the pores of the matrix [10].

Pore size distribution (PSD) curves give important information about the micro- and nanopores that are not easily visible by means of optical microscopy. The main peak obtained in the PSD curves of mortars corresponds to radius of pores comprised between 0.1 and 1 μm (Fig. 4). This is a structural peak typical of lime pastes and it can appear more or less shifted in the x axis, depending on the amount of water added during mixing [13].

The same pores size distribution is maintained after 2 years of carbonation although there is a decrease in the amount of pores with radii comprised between 0.1 and 1 μm (Fig. 4). Since MIP analysis only detects interconnected pores, the volume reduction of pores of the same size indicates that the interconnection among these pores decreases. This occurs due to calcite crystallization during the carbonation process [19].

Apart from porosity, the micro-characteristics of mortars are defined by the form of the mineral phases present in the matrix, namely if they appear in agglomerates or in single particles, as well as their shape and size.

Mortars matrix is mainly characterized by agglomerates of particles, which consist in portlandite crystals and agglomerate, as well as in new formed calcite crystals (Fig. 5) that occasionally surround the aggregate grains (Fig. 5b, f). This calcite has precipitated under semi-crystalline or amorphous particles that have maintained the aspect (in form and size) of the

Table 2 Average values of open porosity (P_o, in %) determined by MIP of mortars after 15 and 60 days and 2 years (730) from their elaboration

Mortar name	Age	P_o
CC1:2	15	41.0
	60	40.8
	730	35.7
CC1:3	15	35.2
	60	35.0
	730	35.7
CC1:4	15	34.5
	60	34.3
	730	31.1
CC1:6	15	30.0
	60	32.1
	730	27.9
CD1:3	15	34.5
	60	36.0
	730	32.7
CS1:3	15	37.8
	60	34.2
	730	35.1

Standard deviation of open porosity values ranges between 0.05 and 3.50

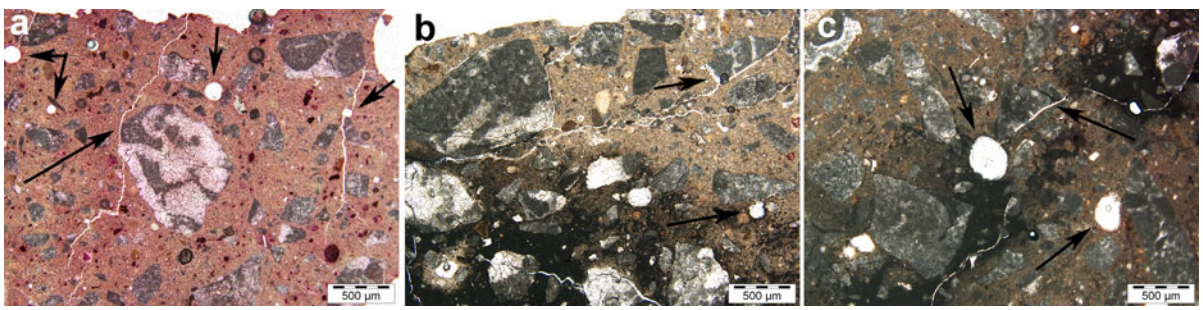

Fig. 2 Optical images taken at the same magnification with plane polars. Large pores and shrinkage fissures in CC1:2 (**a**), CC1:4 (**b**) and CC1:6 (**c**) are indicated by the *arrows*

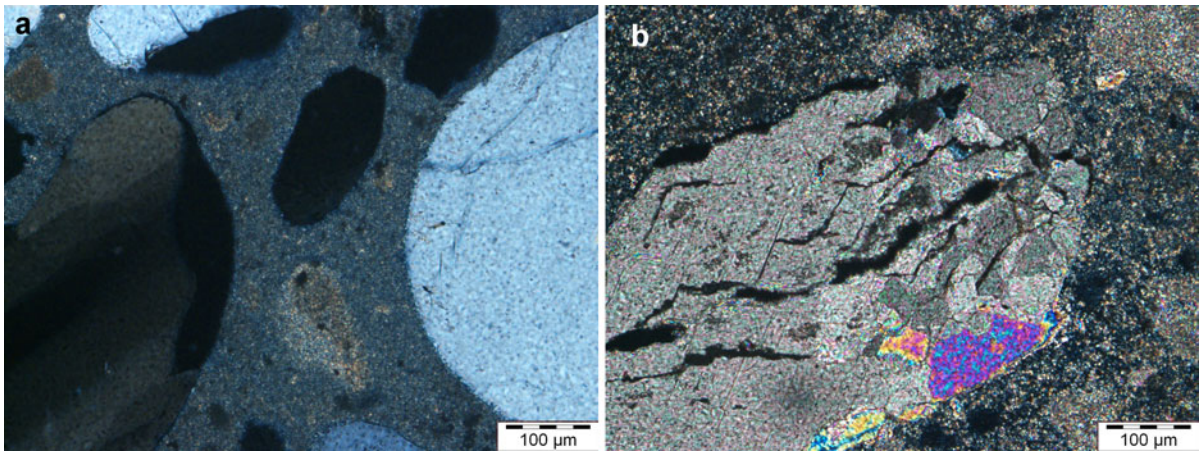

Fig. 3 Optical images taken at the same magnification with crossed polars. Morphology of the aggregates: **a** grain of siliceous aggregate, with rounded and smooth surface, in which no internal porosity appears; **b** grain of calcareous aggregate with irregular edges and rough surface, which presents a big internal porosity and some fissures parallel to the exfoliation planes of calcite

original component of the mortars matrix. In fact, there is a similarity between these particles and both the polydisperse aggregates of microsized particles (about 1 µm in size) of the calcitic lime (Fig. 6a), and the finest fraction of the calcareous aggregate (Fig. 6b).

The precipitation of calcite is especially favoured in nucleation sites of the aggregate when it is characterized by grains with angular shape and rough surface [20], such as the case of the calcareous aggregate. This increases the cohesion in the zone between mortar grains and matrix (interfacial transition zone, ITZ). The optical and electronic observations performed on mortars with aggregates of different mineralogy (CC and CS) agree with this finding. In fact, a worse cohesion was observed in the ITZ of CS1:3 (Fig. 5f), compared to the other mortars prepared with calcareous aggregate (CC and CD). The grains of the siliceous aggregate have rounded shape and smoothed surface (Fig. 3a) that do not favour the joining with new-formed phases and create a zone of disconnection between aggregate and matrix. In addition to the grain morphology, the heterogeneous textural properties of CS mortars are provided also by the different mineralogy and hardness of the mineral phases present in the matrix and in the grain (calcite/portlandite and quartz, respectively). On the contrary, in mortars prepared with calcareous aggregate there is a compositional continuity that may enhance the transformation of portlandite into calcite. Therefore, CA morphology favours the nucleation and growth of the new crystals or amorphous agglomerates of calcite, which often recover the surface of the grains (Fig. 5a, c–e).

3.2 Carbonation degree of the mortars samples

Carbonation of aerial lime mortars is a slow process that involves three main steps: (1) CO_2 diffusion within the mortars; (2) $Ca(OH)_2$ and CO_2 dissolution in the pore water; (3) precipitation of $CaCO_3$ [10]. The carbonation degree depends both on curing conditions (RH and T are two controlling factors, [10, 21, 22]) and on the microcharacteristics of the mortar system (i.e. porosity). Here, curing conditions were the same for all mortars (see Sect. 2.1), so that any variation in the carbonation degree has to be attributed to the intrinsic properties of mortars. The carbonation curves (Fig. 7) present three slopes: a rapid increase of the carbonation degree index (I_{CD}) during the first month, when about half of the portlandite has turned into calcite; a slower increase of I_{CD} in the second month (60–65 %) and a final section in which I_{CD} undergoes a very slight increase (I_{CD} after 2 years is around 70 %). The final values of carbonation degree suggest that among the studied mortars, those prepared with calcareous aggregate (CC and CD mortars) are the most carbonated whilst CS1:3 is the least carbonated at all time intervals. This result can be linked with the compositional and morphological discontinuities that are present in CS and do not favour carbonation, according to our previous considerations (see Sect. 3.1).

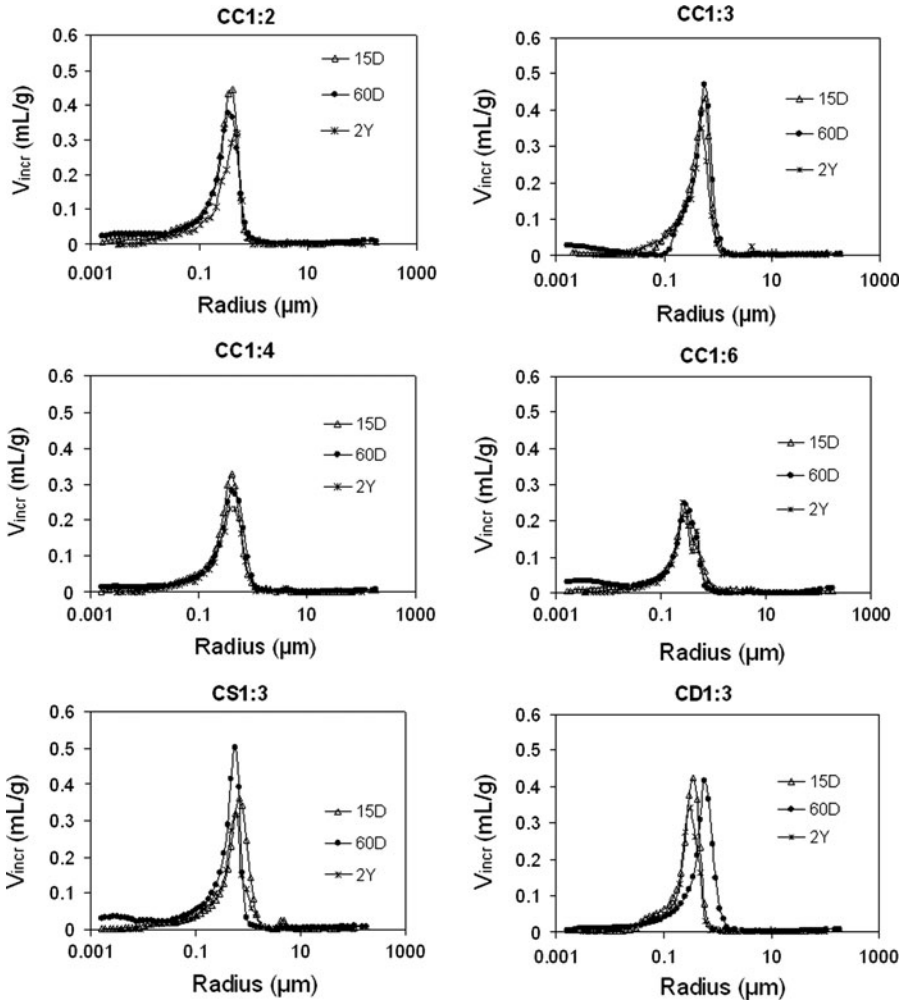

Fig. 4 Pores size distribution curves of CC1:2 (**a**), CC1:3 (**b**), CC1:4 (**c**), CC1:6 (**d**), CD1:3 (**e**) and CS1:3 (**f**) mortar samples after 15 days (15D), 60 days (60D) and 2 years (2Y) since their elaboration

Among CC mortars, CC1:6 is the most carbonated one followed by CC1:2, whilst CC1:3 and CC1:4 present the lowest carbonation degree of their group. CD1:3 mortar, which was one of the least carbonated at the beginning of the study (after 7 days since mortar elaboration), achieves after 2 years the same I_{CD} value than CC1:6.

3.3 Ultrasonic response

3.3.1 Influence of components dosages on ultrasounds

Table 3 shows both the v_p and α_s values measured in mortar samples with different components dosage.

Lime mortar can be considered ideally as a two-phase media constituted by aggregate grains surrounded by a porous matrix. The ultrasonic wave propagation is different in both phases, and the final registered v_p value depends on the particular wave velocity of matrix and aggregate, as well as on the relative volume content of each component in the sample. Differences in both matrix and aggregate velocities (V_p^m and V_p^a, respectively) are due basically to differences in the pore content and, in some cases, in mineralogy, considering constant other parameters such as crystal and pore size.

It has been possible to determine V_p^a measuring it directly on a stone sample of the quarry from which the calcareous aggregate is obtained. This stone is a micritic limestone with very low porosity (< 2 %). The value of v_p measured in this stone was 6,120 m/s.

According to previous studies [2], the wave velocity increases when calcareous aggregate is added to the lime paste. This increase is higher in mortars with

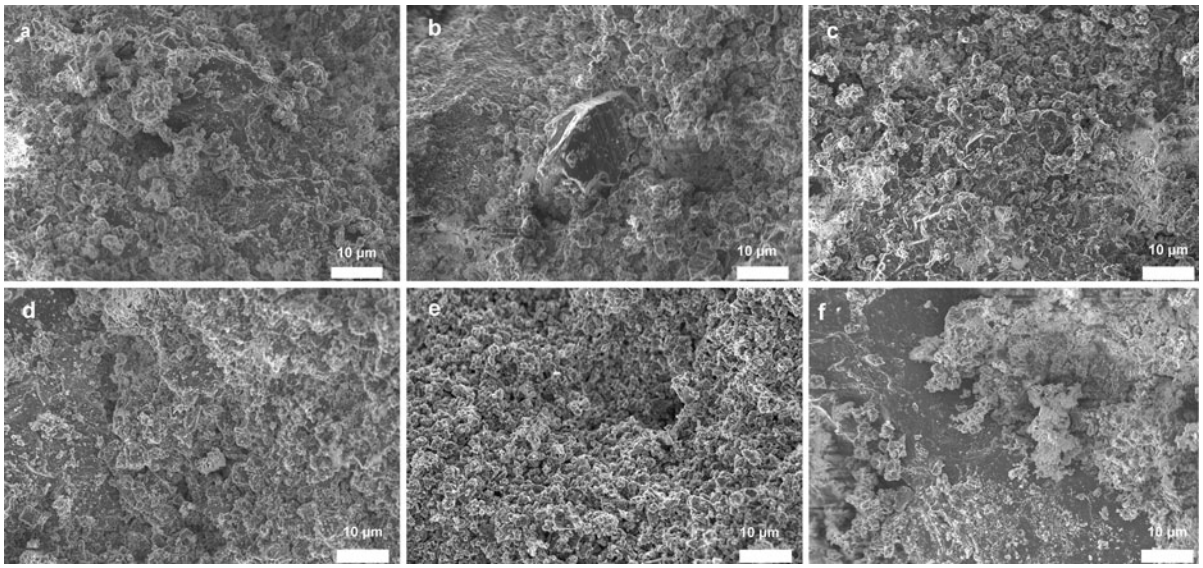

Fig. 5 FESEM images of the mortars after 15 days of carbonation: CC1:2 (**a**), CC1:3 (**b**), CC1:4 (**c**), CC1:6 (**d**), CD1:3 (**e**) and CS1:3 (**f**)

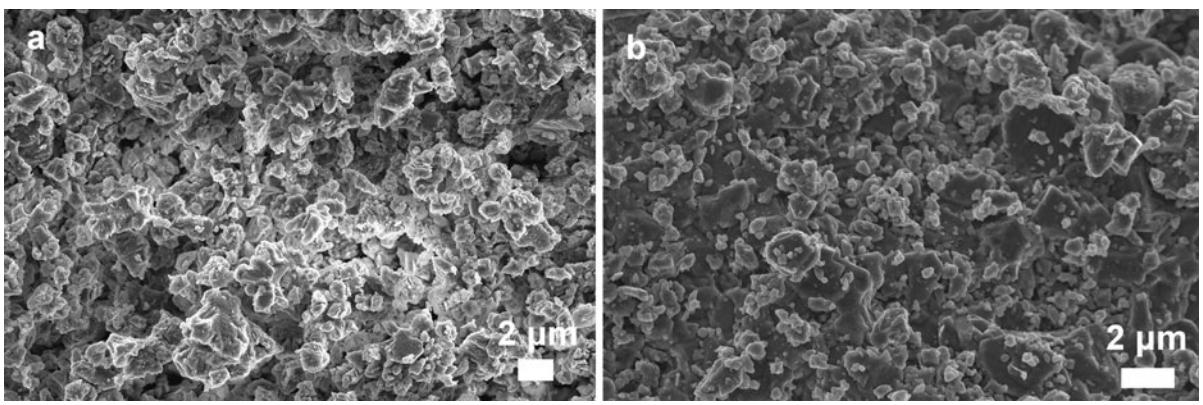

Fig. 6 FESEM images of the calcitic dry hydrated lime (CL) (**a**) and of the fine fraction of the aggregate (**b**)

higher aggregate content. The obtained data in the present work (Table 3) seems to corroborate the general trend shown in bibliography. v_p is higher when the aggregate content in the mortar increases, varying from 1,255 to 1,492 m/s between CC1:2 and CC1:6, respectively (at 15 days since mortar elaboration). However, CC1:3 is an exception in this general trend, since this mortar has a higher aggregate content than CC1:2 but a lower ultrasonic velocity. This finding suggests that the aggregate content in lime mortars is not the most important factor controlling ultrasonic propagation, as it will be discussed below.

3.3.2 Acoustic impedances and wave reflection

The low significance of aggregate content on v_p is related to the strong differences between both matrix and aggregate acoustic impedance. This parameter (acoustic impedance, Z) represents the opposition to the flow of sonic wave through a material, and it is dependent on the density of the material in which wave propagates through. Numerically, acoustic impedance is quantified by:

$$Z = \rho \cdot c \tag{2}$$

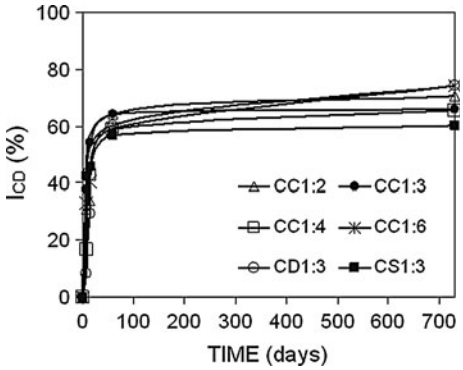

Fig. 7 Carbonation curves of the six mortars. I_{CD} (%) is the carbonation degree index, estimated considering the decrease in portlandite content in time, which was determined by means of XRD quantitative analysis

where Z is the characteristic acoustic impedance, ρ is the density of the medium, and c is the ultrasonic wave velocity. When an ultrasonic wave crosses an interface between two media with different acoustic impedance, the wave divides in two components: a transmitted and a reflected wave. The amount of reflected and transmitted wave depends on the impedance of each one of the media, and it is quantified by the reflection coefficient, R:

$$R = \frac{Z_2 - Z_1}{Z_2 + Z_1} = \frac{\rho_2 V_2 - \rho_1 V_1}{\rho_2 V_2 + \rho_1 V_1} \quad (3)$$

where Z, ρ and V are the impedance, bulk density and ultrasonic wave velocity of the first and second medium (subscripts 1 and 2, respectively).

The R value varies between -1 and 1. An absolute value of R close to 1 indicates that the ultrasonic wave is completely reflected and no fraction of the incident wave will be propagated to the second medium. An absolute value of R close to 0 indicates instead that a higher wave fraction will be transmitted and a small part will return as reflected wave.

By analyzing the aggregate surroundings in mortars from an acoustic point of view, the aggregate surface constitutes an interface which separates two media with different impedance. The aggregates have an average bulk density of 2.66 g/cm^3 and an average v_p of 6,200 m/s, but it is not possible to know exactly the density and the propagation velocity values of the mortar matrix. In order to obtain a critical value of impedance, matrix is considered as an ideal homogeneous material without porosity (unreal conditions). Under these conditions, matrix density is 2.24 g/cm^3 (corresponding to the portlandite density) and V_p^m is 6,750 m/s (propagation velocity through an ideal portlandite crystal). Considering these values, the acoustic impedances of both aggregates and the ideal matrix are 19.77 and 15.12 MPa s/m, and the reflection coefficient for a wave travelling from the aggregate to the matrix results of -0.13. A reflection

Table 3 Average and standard deviation values of v_p (in m/s) and α_s (in dB/cm) measured in the mortar types studied at different interval times

	Time (days)	Mortar name					
		CC1:2	CC1:3	CC1:4	CC1:6	CD1:3	CS1:3
v_p	8	930±43	772±34	1015±53	1212±73	1093±57	792±36
	10	1033±61	847±75	1142±58	1356±52	1252±51	882±41
	15	1255±53	1064±40	1307±57	1492±70	1317±67	1052±43
	28	1512±52	1295±38	1641±54	1795±63	1611±65	1320±43
	60	1693±78	1379±38	1729±44	1873±75	1719±35	1406±32
	730	1898±58	1452±29	1885±60	2090±97	1875±30	1553±35
α_s	8	1.47±0.13	1.63±0.20	1.43±0.14	1.39±0.15	1.17±0.21	1.52±0.10
	10	1.43±0.11	1.59±0.16	1.44±0.17	1.36±0.16	1.23±0.18	1.49±0.11
	15	1.23±0.16	1.43±0.14	1.31±0.16	1.26±0.17	1.13±0.15	1.33±0.09
	28	1.10±0.15	1.32±0.12	1.25±0.17	1.16±0.14	0.10±0.16	1.25±0.05
	60	1.09±0.09	1.19±0.11	1.22±0.23	1.08±0.13	0.97±0.96	1.23±0.10
	730	0.99±0.05	1.16±0.10	1.19±0.07	1.05±0.10	0.99±0.26	1.27±0.10

coefficient of 0.13 indicates that around 13 % of the incident wave is reflected and only 87 % of the wave is propagated in every aggregate-matrix contact. This value is a critical (optimum) approximation considering the most favourable conditions for the wave propagation (ideal homogeneous matrix without porosity and wave transmission through straight interfaces). However, if more real characteristics are supposed for mortar matrix, such as a matrix bulk density of 1.57 g/cm^3 (considering a matrix porosity of 30 %) and a propagation velocity of 2,000 m/s (closer to the total mortar v_p), a reflection coefficient of −0.68 is obtained. It means that when ultrasonic waves go from the aggregate to the matrix, 68 % of the incident wave is reflected and only a small component of the initial wave is propagated into the matrix.

Taking into account any of both situations (ideal or real matrix characteristics), it is clear that the ultrasonic wave is strongly attenuated when it propagates from the aggregate grains to the matrix, and consequently, the final received signal at the end of the mortar sample corresponds mainly to the wave propagated through the matrix. The final wave velocity will depend mainly on the mineralogy and the porosity of the matrix. In particular, the latter will be the main factor controlling the scattering of the wave, since the higher porosity the higher the wave delay.

At the beginning of Sect. 3.3.1, a direct relationship between mortar aggregate content and v_p was found. This can seem a contradiction after our previous discussion, in which it is demonstrated that the aggregate has not a significant influence on v_p. Effectively, the connection between mortar dosage and v_p is not due to the aggregate content, but to the initial quantity of water added to the mortar mixture in order to obtain an optimum workability (kneading water). The lower the binder content in the mortar, the lower the kneading water (Table 1).

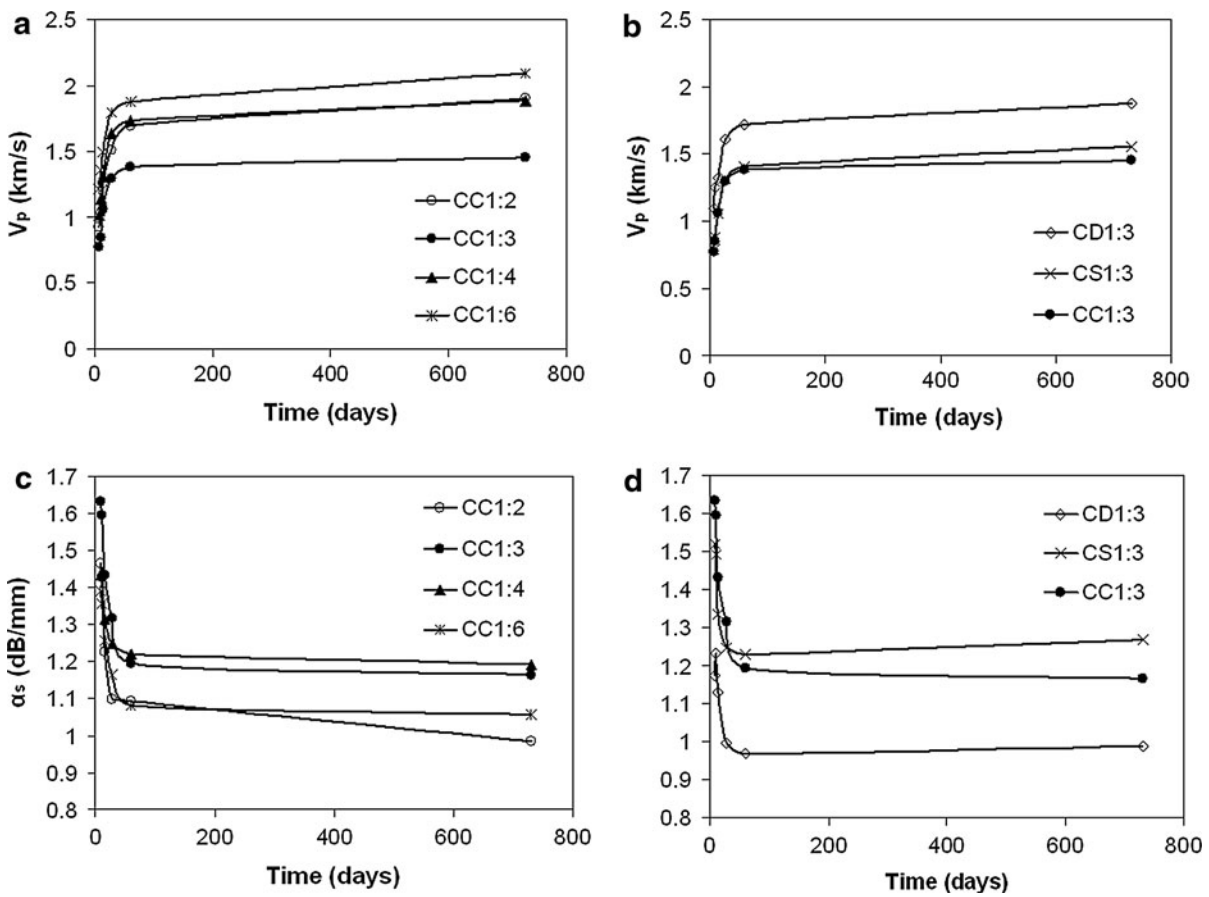

Fig. 8 Propagation velocity (v_p) (**a**, **b**) and spatial attenuation (α_s) (**c**, **d**) of ultrasonic waves during the carbonation process

Mortars with low kneading water result in samples with less porous matrix, and consequently, they present better characteristics to the wave propagation.

When the relationship between mortar aggregate content and v_p was studied at the beginning of Sect. 3.3.1, CC1:3 was an exception since this mortar had a higher aggregate content than CC1:2 but a lower ultrasonic velocity. Now it is possible to understand the apparently anomalous behaviour of CC1:3, attending to the amount of kneading water employed in each case. Table 1 shows that CC1:3 is the mortar with the highest content of kneading water (higher than CC1:2 and CC1:4), and consequently, it has the most porous matrix and the worst characteristics to ultrasonic propagation.

3.3.3 *Influence of aggregate content and kneading water on spatial attenuation*

Values of spatial attenuation are very similar in all mortar types (Table 3). However, a small α_s decrease is observed when the aggregate content of mortars increases. This trend is valid for all samples except for CC1:3 in which it was measured a higher wave attenuation than in CC1:2, although CC1:3 has a bigger aggregate content. As discussed above, differences between mortars are not mainly due to aggregate content, but to the water content. Since CC1:3 is the mortar with the highest water content, and consequently with the most porous matrix, it is predictable that it will be the mortar with the highest wave attenuation values.

Ultrasonic waves can be attenuated by several causes, such as absorption in each of the individual phases, visco-inertial losses due to density discrepancies of the constituent materials, thermal dissipation losses, and scattering [23]. Several works demonstrate that scattering is the most important causes involving wave attenuation in mortars [2, 3, 24]. Those studies also demonstrate that the aggregate content has a direct relationship with the wave attenuation due to this phenomenon (the higher the aggregate content, the higher the wave attenuation), and a higher w/c (higher porosity) logically gives place to higher values of the attenuation parameter. In the mortars studied in this paper, the effect of one type of inclusions (pores or aggregate) on wave scattering is offset by the effect of the other one, given that CC1:6 is the mortar with the highest aggregate content, the lowest water content, and consequently, the lowest matrix porosity, whilst the samples with the lowest aggregate content (CC1:2 and CC1:3) are mortars with high w/c ratio. The result is that the water content has a slightly bigger influence on the total wave scattering than the aggregate content in mortars with similar α_s.

3.3.4 *Influence of aggregate mineralogy and grading on ultrasounds*

In order to evaluate the influence of aggregate mineralogy and grading on v_p and α_s three different mortars have been studied (CC1:3, CD1:3 and CS1:3) which have the same dosage (Table 1), but different grading (CC1:3 and CD1:3) or aggregate mineralogy (CD1:3 and CS1:3) (see Sect. 2.1 for mortars characteristics). Table 3 shows the measured v_p and α_s in these mortars. Aggelis and Philippidis [2] assert that the grains size is very important in wave attenuation. In their study, mortars prepared with coarse aggregate exhibit greater attenuation than mortar with fine aggregate. This result is coherent with the data shown in this paper, where CC1:3 has the biggest aggregate sizes and the highest α_s value (1.63 dB/mm). However, CC1:3 has also a higher water content than CD1:3 (i.e. a higher porosity) and consequently it is not possible to distinguish the weight of the effect of both variables on α_s.

With respect to the influence of grading on wave velocity, no evidences have been found about the dependence of v_p and aggregate size. Previous studies [1] do not show any relationship between both variables, and no apparent connection seems to exist between them according to the results obtained in this paper. The v_p increase observed in data (from 772 to 1,093 m/s in CC1:3 and CD1:3, respectively) is related to the lower water content of CD1:3, which causes a lower porosity in the matrix.

Another important aspect is the influence of aggregate mineralogy on both v_p and α_s. In this case, CD1:3 and CS1:3 are composed by aggregates with the same grading (discontinuous) and the same dosage, but different mineralogy (calcareous and siliceous, respectively). Differences in both ultrasonic parameters are observed, showing that the siliceous mortar presents the lowest wave velocity and the highest spatial attenuation. Although quartz has a lower ultrasonic P-wave velocity than calcite (6,060 and 6,650 m/s, respectively, after Schön [1]), which

could cause a slower propagation of the wave through the mortar with siliceous aggregate, differences on aggregate mineralogy can not explain significant variations on v_p and α_s due to the fact that ultrasonic wave is strongly attenuated after its propagation through aggregates (see Sect. 3.3.1). Consequently, the causes of ultrasonic variations between siliceous and calcitic mortars have to be related to matrix characteristics.

The quantity of initial water added to the mixture is almost the same in both mortars (27 and 26.5 % in CD1:3 and CS1:3, respectively), so the matrix porosity can be considered practically the same, and therefore, it can not explain the differences in ultrasonic behaviour.

However, there is a strong difference in the pores located at the interfacial zone (ITZ, the zone between the matrix and the surface of grains) of the two mortars. As explained in Sect. 3.1, mortars prepared with calcareous aggregates have a textural continuity between matrix and aggregate grains, whilst mortars with siliceous aggregate show some porosity developed at the matrix-aggregate contact. These differences in the ITZ can explain the variations observed in the ultrasonic parameters since a higher nucleation of calcite in the matrix surrounding the aggregate grains offers a slightly more continuous interface between aggregate and matrix, thus favouring the ultrasonic propagation and decreasing the proportion of reflected wave. This certain continuity between aggregate and matrix is exclusive of lime mortars with calcareous aggregates, whilst the low cohesion at the ITZ found in CS1:3 contributes to increase the wave reflection, getting more difficult the propagation of ultrasonic pulses. This relationship between low-cohesion in the ITZ and increase of the ultrasonic attenuation was also observed by Chekroun et al. [24].

3.3.5 *Influence of carbonation degree on ultrasounds*

Figure 8 shows the time evolution of both v_p and α_s during the carbonation process. In these graphs it is possible to observe the mechanical improvement of mortars due to the textural and mineralogical changes led by carbonation. All mortars suffer an increase of v_p and a decrease of α_s and they show parallel trends: a rapid v_p increase and α_s decrease during the first 60 days and a quasi no variation of v_p and α_s (respectively) from 60 days to 2 years.

As explained above, two main changes are produced in mortar during the carbonation process: on the one hand, the mineralogical transformation of portlandite into calcite and, on the other hand, the matrix porosity reduction. The first change is responsible for the rapid changes in the ultrasonic response in the first

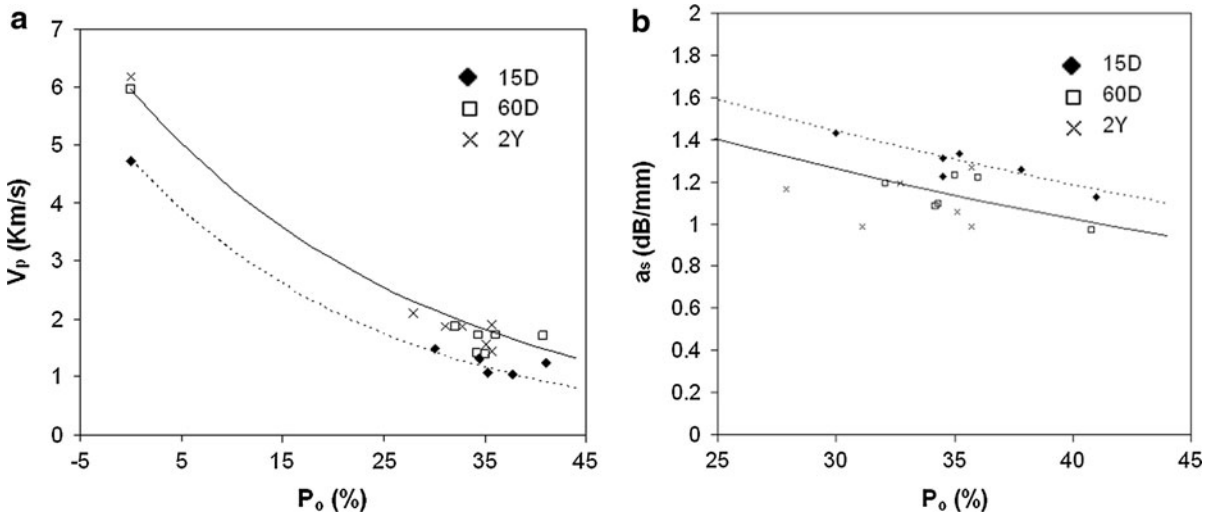

Fig. 9 Relationship between porosity, carbonation degree and ultrasonic response, where the open porosity (P_o) is represented as function of the velocity of propagation (v_p) (**a**) and the spatial attenuation (α_s) (**b**) of ultrasonic waves. Solid and dot lines represent the exponential (**a**) and lineal (**b**) fitting of high and low-carbonated mortars, respectively. The equations obtained from the fitting curves in (**a**) and (**b**) are indicated in the text as Eqs. 6 and 8, respectively. *15D* 15 days; *60D* 60 days; *2Y* 2 years of carbonation

60 days. It has been found that carbonation degree increases rapidly in the first moments of the mortar life, reaching about the 70 % of the total carbonation in only 2 months.

The transformation of portlandite into calcite leads to important elastic considerations. It is known that the velocity of the ultrasonic wave propagation through minerals depends directly on two elastic constants: the Young's Modulus (E) and the Poisson's ratio (μ) of the mineral. These relations are mathematically expressed after Eqs. 4 and 5:

$$v_p = \sqrt{\frac{E(1-\mu)}{\rho(1+\mu)\cdot(1-2\mu)}} \quad (4)$$

$$v_s = \sqrt{\frac{E}{2\rho(1+\mu)}} \quad (5)$$

E in portlandite and calcite is 41.7 and 88.19 GPa, respectively (after data published in Speziale et al. [25], for portlandite and Schön [1], for calcite), whilst $\mu_{portlandite}$ and $\mu_{calcite}$ are 0.25 and 0.316, respectively. Taking into account that $\rho_{portlandite} = 2.24$ g/cm^3 and $\rho_{calcite} = 2.71$ g/cm^3, the P-wave velocity in a pure crystal of portlandite and calcite will be 4,726 and 6,779 m/s, respectively. Therefore, the acceleration of P-waves during the first weeks can be completely explained by the carbonation degree of the sample. Moreover, a reduction of the porosity in the mortar matrix is also observed during the carbonation process and this fact contributes further to improve the ultrasonic propagation through mortar.

3.3.6 *Quantitative approach to textural influence on ultrasonic propagation*

According to previous discussions, ultrasonic wave propagation on lime mortars is mainly influenced by two textural parameters: the porosity of the matrix and the carbonation degree, remaining independent of other aspects such as aggregate mineralogy or grading.

Figure 9 shows the average values of v_p and α_s of each mortar type according to their porosity and their age since preparation (15 days, 60 days and 2 years). Moreover, three additional points are added in the v_p–P_o graph. These points have been calculated from theoretical considerations and correspond to three ideal mortars without porosity ($P_o = 0$ %). Propagation velocity at these ideal materials was calculated from the specific velocity of each constituent mineral (6,750 and 7,290 m/s for portlandite and calcite, respectively) knowing their abundance at different ages after the XRD data.

It has been possible to obtain two line fitting from each graph, finding a numerical relationship between the ultrasonic parameters and both porosity and carbonation degree. Dot lines show the relationship between ultrasonic parameters and porosity for low-carbonated mortars (measures were carried out 15 days after mortar preparation). Solid line shows the relationship for high-carbonated mortars. In the case of v_p, measures at 60 days and 2 years fall on the same line, showing a unique trend. In the case of α_s, solid line is fitted only for data at 60 days because values at 2 years appear scattered and no correlation can be established.

We obtained the following empirical equation for v_p, as function of mortar porosity and carbonation degree:

$$v_p = v^m \cdot e^{\frac{-x}{100}\left(4.2-\frac{I_{CD}}{100}\right)} \quad (6)$$

where x is the porosity (in %) and I_{CD} is the carbonation degree index. v^m is the theoretical velocity obtained from the mineralogical composition of mortar (calculated by XRD) and the characteristic ultrasonic velocity of each constituent mineral. This value (v^m) was obtained by using a second empirical equation:

$$v^m = v_p^p \cdot \chi^p + v_p^c \cdot \chi^c \quad (7)$$

where, χ^p and χ^c, v_p and v^c are the relative volumes and specific ultrasonic velocity (respectively) of portlandite and calcite (p and c, respectively).

A third empirical equation was obtained for α_s, as function of mortar porosity and carbonation degree:

$$\alpha_s = (2.58 - 0.32 I_{CD}) \cdot e^{x\left(\frac{-1.95-0.231 I_{CD}}{100}\right)} \quad (8)$$

where x is the porosity (in %) and I_{CD} is the carbonation degree index.

Although these equations are supported by numerous data, it will be necessary to develop a higher amount of tests and measurements in the future in order to confirm the trends and equations obtained in this paper.

4 Conclusions

The aim of this study was to investigate the influence of the textural characteristics of different aerial lime-

based mortars on the propagation velocity and the spatial attenuation of P waves. Six types of mortars were studied and divided in two main groups: the first one composed by four mortars of the same composition and different binder-to-aggregate ratios, and the second one constituted by three mortars prepared with the same binder-to-aggregate ratio but different aggregate characteristics. In this second group, two aggregates with different composition (siliceous and calcareous) and grading (continuous and discontinuous) were used for the preparation of mortars. The mineralogical and textural properties of mortars have been studied for 2 years in order to interpret the ultrasonic response at every interval of time.

Ultrasounds have proved to be a sensitive tool for determining textural characteristics of lime-mortars. Several textural aspects were considered initially as controller factors of the wave propagation through mortars: porosity, binder-to-aggregate ratio, aggregate mineralogy and grading and carbonation degree of mortars. Finally, only two parameters result to be the most significant for ultrasonic propagation: matrix porosity and carbonation degree.

Textural parameters related to the aggregate (mineralogy, grading and aggregate content) result little influential on wave propagation velocity (v_p) and spatial attenuation (α_s). This fact is due to the strong differences in acoustic impedance between both mortar matrix and aggregates. Aggregates are obtained from a very low-porous limestone (porosity lower than 2 %) and considerably high bulk density (around 2.66 g/cm^3). As a result, the propagation velocity of waves through aggregates is high (6,200 m/s), and, consequently, its acoustic impedance is high too (around 19.77 MPa s/m). On the contrary, mortar matrix has high porosity ($\sim$30 %), low bulk density and presumably low ultrasonic propagation velocity. The matrix acoustic impedance is estimated at 4 MPa s/m. This difference between acoustic impedances causes a strong reflectance of the ultrasonic wave when it is propagated from aggregate to matrix. Accordingly, the registered wave at the end of the mortar sample corresponds mainly to the front wave propagated through the mortar matrix, and therefore the waveform is a result of the matrix characteristics.

In accordance with previous reasoning, v_p and α_s are a reflection of the porosity and mineralogy of the mortar matrix. The first one is related to the amount of kneading water added during mortar preparation, whilst the second one is dependent on the age of lime mortar. The whole water content evaporates producing pores in the mortar matrix, and, consequently, causing wave delay and scattering. The most porous mortars present the lowest v_p and the highest α_s values. The carbonation process, for its part, causes a mineralogical transformation of the matrix as well as a slight porosity reduction (both factors favour the wave propagation). A high-carbonated matrix (characterized by a high content of calcite) has better elastic characteristics than low-carbonated matrix (with a predominant content of portlandite), and hence, the wave propagation is more favoured in the first one.

Finally, all these results have been integrated in numerical equations that allow assessing the textural characteristics of lime mortars from v_p and α_s measurements.

This study constitutes a useful approximation for the evaluation of lime mortars texture by means of non-destructive tests, which is in many cases a crucial point, such as in the field of Cultural Heritage.

Acknowledgments This study was financially supported by Research Group RNM179 of the Junta de Andalucía and by the Research Project P09-RNM-4905. We thank the revision of an anonymous referee, as well as Jason Weiss for his useful suggestions.

References

1. Schön JH (1996) Physical properties of rocks: fundamentals and principles of petrophysics. Handbook of geophysical exploration, Sect I, seismic exploration, vol 18. Pergamon, New York
2. Aggelis DG, Philippidis TP (2004) Ultrasonic wave dispersion and attenuation in fresh mortar. NDT&E Int 37:617–631
3. Lafhaj Z, Goueygou M (2009) Experimental study on sound and damaged mortar: variation of ultrasonic parameters with porosity. Constr Build Mater 23:953–958
4. Mishra SR, Kumar S, Park A, Rho J, Losby J, Hoffmeister BK (2003) Ultrasonic characterization of the curing process of PCC fly ash-cement composites. Mater Charact 50:317–323
5. Goueygou M, Lafhaj Z, Soltani F (2009) Assessment of porosity of mortar using ultrasonic Rayleigh waves. NDT&E Int 42:353–360
6. Voigt T, Sun Z, Shah S (2006) Comparison of ultrasonic wave reflection method and maturity method in evaluating early-age compressive strength of mortar. Cem Concr Compos 28:307–316
7. Cazalla O, Sebastián E, Cultrone G, Nechar M, Bagur MG (1999) Three-way ANOVA interaction analysis and ultrasonic testing to evaluate air lime mortars used in cultural heritage conservation projects. Cem Concr Res 29:1749–1752

8. Molero M, Segura I, Hernández MG, Izquierdo MAG, Anaya JJ (2010) Characterization of mortar samples using ultrasonic scattering attenuation. Phys Procedia 3(1):839–845
9. Molero M, Segura I, Hernández MG, Izquierdo MAG, Anaya JJ (2011) Ultrasonic wave propagation in cementitious materials: a multiphase approach of a self-consistent multiple scattering model. Ultrasonics 51(1):71–84
10. Moorehead DR (1986) Cementation by the carbonation of hydrated lime. Cem Concr Res 16:700–708
11. Rodriguez-Navarro C, Cazalla O, Elert K, Sebastian E (2002) Liesegang pattern development in carbonating traditional lime mortars. Proc R Soc London 458:2261–2273
12. Cazalla O, Rodriguez-Navarro C, Sebastian E, Cultrone G (2000) Aging of lime putty: effects on traditional lime mortar carbonation. J Am Ceram Soc 83(5):1070–1076
13. Arandigoyen M, Pérez Bernal JL, Bello López MA, Alvarez JI (2005) Lime-pastes with different kneading water: pore structure and capillary porosity. Appl Surf Sci 252:1449–1459
14. UNE-EN 459-1 (2002) Description building lime—Part 1: definitions, specifications and conformity criteria. AENOR, Madrid
15. UNE-EN 1015-3 (1998) Methods of test for mortar for masonry. Determination of consistence of fresh mortar (by flow table). AENOR, Madrid
16. Martín Ramos JD (2004) XPowder. A software package for powder X-ray diffraction analysis. Lgl. Dep. GR 1001/04
17. UNE-EN 14579 (2005) Natural stone test methods. Determination of sound speed propagation. Spanish Association for Standardisation and Certification (AENOR), Madrid
18. Martínez-Martínez J, Benavente D, García-del-Cura MA (2011) Spatial attenuation: the most sensitive ultrasonic parameter for detecting petrographic features and decay processes in carbonate rocks. Eng Geol 119:84–95
19. Cultrone G, Sebastián E, Ortega Huertas M (2005) Forced and natural carbonation of lime-based mortars with and without additives: mineralogical and textural changes. Cem Concr Res 35:2278–2289
20. Lanas J, Alvarez-Galindo J (2003) Masonry repair lime-based mortars: factors affecting the mechanical behaviour. Cem Concr Res 33(11):1867–1876
21. Van Balen K (2005) Carbonation reaction of lime, kinetics at ambient temperature. Cem Concr Res 35:647–657
22. Houst YF, Wittmann FH (1994) Influence of porosity and water content on the diffusivity of CO_2 and O_2 through hydrated cement paste. Cem Concr Res 24(6):1165–1176
23. Barton N (2007) Rock quality, seismic velocity, attenuation and anisotropy. Balkema, London
24. Chekroun M, Le Marrec L, Abraham O, Durand O, Villain G (2009) Analysis of coherent surface wave dispersion and attenuation for non-destructive testing of concrete. Ultrasonics 49:743–751
25. Speziale S, Reichmann HJ, Schilling FR, Wenk HR, Monteiro PJM (2008) Determination of the elastic constants of portlandite by Brillouin spectroscopy. Cem Concr Res 38:1148–1153